ever, it is believed that polarization needs several tens of a nanosecond to develop. Thus it may be possible to use CIDNP NMR to study the inhomogeneous reactions of radiation chemistry ("spurts", etc.).

Despite their differences, the common feature of both magnetic polarization methods, CIDEP and CIDNP, is that each reveals in its own fashion the memory of radical interactions in solution.[17] As a result, in addition to the many facets of solution microdynamics which are revealed, both techniques can be superb tools for the study of radical reaction mechanisms in solution. This is especially true in radiation chemistry where it may be possible to show that the polarization-producing pathways can quantitatively reflect the bulk of radical reactions in solution.

Acknowledgments. This work could not have been possible without the expert help of K. W. Johnson in all aspects of instrument design. We wish to thank the operators of the Argonne Van de Graaff, R. H. Lowers and A. Youngs, for their efforts.

References and Notes

(1) Work performed under the auspices of the U.S. Energy Research and Development Administration.
(2) Paper I: A. D. Trifunac, K. W. Johnson, and R. H. Lowers, *J. Am. Chem. Soc.*, **98**, 6067 (1976).
(3) Summer faculty research participant at ANL.
(4) General references. M. S. Matheson and L. M. Dorfman, "Pulse Radiolysis", MIT Press, Cambridge, Mass., 1969. J. W. T. Spinks and R. J. Woods, "An Introduction to Radiation Chemistry", 2nd ed, Wiley-Interscience, New York, N.Y. 1976.
(5) R. W. Fessenden, *J. Chem. Phys.*, **58**, 2489 (1973).
(6) A. D. Trifunac and M. C. Thurnauer, *J. Chem. Phys.*, **62**, 4889 (1975).
(7) A. D. Trifunac, K. W. Johnson, B. E. Clifft, and R. H. Lowers, *Chem. Phys. Lett.*, **35**, 566 (1975).
(8) A. R. Lepley and G. L. Closs, Ed., "Chemically Induced Magnetic Polarization", Wiley-Interscience, New York, N.Y., 1973.
(9) G. L. Closs and A. D. Trifunac, *J. Am. Chem. Soc.*, **92**, 2183 (1970).
(10) R. Kaptein, *Chem. Commun.*, 732 (1971); A. D. Trifunac, Ph.D. Thesis, Chicago, Ill., 1971.
(11) The exchange coupling (J) is usually quite small and thus considered unimportant in CIDNP.[12] However, the observation of CIDEP in these systems indicates that J is not zero.
(12) G. L. Closs, *Adv. Magn. Reson.*, **7**, 157 (1974).
(13) R. G. Lawler and M. Halfon, *Rev. Sci. Instrum.*, **45**, 84 (1974).
(14) J. A. Wargon and F. Williams, *J. Am. Chem. Soc.*, **94**, 7917 (1972).
(15) J. A. Den Hollander, Ph.D. Thesis, Leiden, 1976; *Chem. Phys.*, **10**, 167 (1975).
(16) The observation of polarization in the products of radicals that undergo a nonreactive encounter with e_{aq}^-, before they encounter H radical to give products, illustrates the carry over of polarization. This has been discussed in some detail by Den Hollander.[15]
(17) We are investigating whether there is any transfer of polarization between the electron and nuclear spin systems. One of the referees has raised this point concerning the possible cross-relaxation polarization transfer between CIDEP in radicals and CIDNP in their products.
(18) E. C. Avery, J. R. Remko, and B. Smaller, *J. Chem. Phys.*, **49**, 951 (1968); F. P. Sargent and E. M. Gardy, *Chem. Phys. Lett.*, **39**, 188 (1976).
(19) R. W. Fessenden and R. H. Schuler, *J. Chem. Phys.*, **39**, 2147 (1963).
(20) R. Livingston and H. Zeldes, *J. Chem. Phys.*, **44**, 1245 (1966).

Photoelectron Spectra of Solid Inorganic and Organometallic Compounds Using Synchrotron Radiation. Valence Band Spectra and Ligand Field Broadening of Core d Levels

G. M. Bancroft,*[1a] T. K. Sham,[1a] D. E. Eastman,[1b] and W. Gudat[1b]

Contribution from the Chemistry Department, University of Western Ontario, London N6A 5B7, Canada, and the IBM Thomas J. Watson Research Centre, Yorktown Heights, New York 10598. *Received September 3, 1976*

Abstract: Using synchrotron radiation from the Wisconsin storage ring as the photon source, we have obtained valence band and outermost d core level photoelectron spectra of a number of solid Sn, In, Sb, and Pb organometallic and inorganic compounds containing phenyl (Ph), methyl (Me), chloride, and acetylacetonates (AcAc, BzAc, BzBz) as ligands. With a total instrumental resolution of 0.3 eV at 57 eV photon energies, we have obtained d core line widths in the low 0.7 eV region, within 0.15 eV of the corresponding metal line widths. Correlations of the Sn 4d line widths and chemical shifts with previously obtained 3d widths and shifts show that we have minimized experimental difficulties such as charging and decomposition. The resolution in the valence band region is good enough to detect and assign a large number of the valence band peaks. For example, eight valence band peaks can be resolved in the Ph_4Sn spectrum, and these peaks can be assigned readily to the benzene molecular orbitals and the Sn–C bonding orbitals. The routinely variable photon energy is sometimes useful for assigning peaks in these spectra. The broadening of the Sn 4d peaks is attributed to an unresolved ligand field splitting. In particular, the broadening is due to the asymmetry or electric field gradient C_2^0 term in the crystal field expansion. From the known nuclear field gradients, the magnitude of the C_2^0 term (-0.036 ± 0.006 eV) in the Me_2Sn compounds is shown to be consistent with the $|C_2^0|$ values observed previously for Me_2Cd (0.026 eV), XeF_2 (0.042 eV), and XeF_4 (0.043 eV). These results show that the electric field gradient splitting has to be considered as an important broadening mechanism (and splitting mechanism at very high resolutions) in photoelectron and adsorption studies. The 4d and 5d spin–orbit splittings do not vary with the chemical environment. However, the ratio of the $d_{5/2}$:$d_{3/2}$ intensities appears to be sensitive to the chemical environment and varies considerably from the theoretical 1.5:1 ratio expected in an independent particle picture.

Photoelectron spectroscopy has been divided into two distinct areas because of the availability of simple intense light sources. If the photon energy is in the vacuum ultraviolet (VUV) range [for example, He(I) (21.2 eV) or He(II) (40.8 eV)], the technique is often called ultraviolet photoelectron spectroscopy (UPS).[2a] If the photon energy is in the x-ray range [for example, Mg Kα (1253 eV) or Al Kα (1486 eV)], the technique is called x-ray photoelectron spectroscopy (XPS or ESCA).[2b] The former technique has been used predominantly to study valence levels of gases at high instrumental resolution ($\leq$20 meV) and solids at lower resolution ($\leq$0.3 eV), while the latter technique is used normally to study core levels at comparatively low resolution ($\geq$0.6 eV). In the x-ray case, the large line widths usually observed arise mainly from the

source line widths, and it is very important to decrease this source width by monochromatization.[3] Discrete source lines in-between 40.8 and 1253 eV have been developed,[4] but experimental difficulties (source stability, intensity, or line width) have inhibited their widespread use.

Recently, as Eastman has pointed out,[5] the distinction between UPS and XPS has become blurred by the use of synchrotron radiation sources which can span the VUV and x-ray regions. These sources, which provide an intense continuum of linearly polarized radiation, have two main advantages for the chemical spectroscopist. First, after monochromatization, it is possible to obtain considerably better instrumental resolution (with an adequate count rate) than for presently marketed XPS instruments. Second, the routinely variable photon energy enables an optimum photon energy to be chosen to study a given effect and also enables cross sections to be studied as a function of photon energy. These and other advantages of a monochromatized synchrotron source have been discussed (see ref 5 and other articles in the VUV conference).

In this paper we present a study of the valence band spectra and outermost core d levels of solid Sn, In, Sb, and Pb inorganic and organometallic compounds. These results demonstrate some of the advantages of the synchrotron source for studying inorganic solid insulators. Solid insulators have been a particular problem in XPS studies.[6] Charging effects, sample decomposition, and surface impurities have often resulted in broad lines which were difficult to calibrate accurately. The charging effects (and often the associated differential charge broadening) are particularly large when a monochromatized source is employed,[7] and electron flood guns are normally used to compensate for the charging effect. It was one of our main intentions to use our improved resolution and monochromatized source to further our study[8] of extrinsic solid state broadening contributions (for example, from differential charging) so that we would obtain high resolution on both core level and valence band spectra. We were hopeful that the high instrumental resolution ($\leq$0.3 eV) would enable us to clarify ligand field broadening[8,9] and splitting[9] of core levels.

In the first part of this paper, the experimental methods are described. In part II, we describe briefly the variation of cross sections for various orbital symmetries with photon energy in Ph_4Sn. These spectra enable us to choose the optimum photon energy for observing both the core d and valence band peaks at good (0.3 eV) resolution. We demonstrate that both core level widths and valence band widths of nonconductor solids can approach those of metals and gases. The valence band peaks are then assigned to the molecular orbitals in the complexes. In part III, we discuss the observed line broadening of the Sn 4d peaks and show that the major cause of line broadening in these compounds is due to the asymmetric C_2^0 term (the term that transforms like the electric field gradient) in the crystal field expansion. Other recent results are shown to be consistent with this explanation.

(I) Experimental Section

(A) **Apparatus.** The 240 MeV storage ring Tantalus I was employed as the light source. This provides a continuously variable photon flux from the infrared to the far UV. The spectral intensity peaks at about 70 eV. At higher energies, the photon flux drops off rapidly, so that it is difficult to obtain photoelectron spectra at both good resolution *and* high intensity above 100 eV photon energies.

Focusing and monochromatization of the radiation was achieved by the system described earlier.[10] Two monochromators were used: a 1-m Seya Namioka type which covered the photon energies 5 to 40 eV, and a 2-m grazing incidence type which covered the photon energies 40 to 100 eV. Adjustable slits permit the photon resolution $\Delta\lambda$ to be adjusted from $\Delta\lambda$ = 16 to 0.4 Å. Thus typical photon resolutions of ~0.2 eV at 50 eV photon energy and ~0.05 eV at 30 eV are obtained. The monochromatized beam from both monochromators passes through the focal point of a two-stage cylindrical mirror electron energy analyzer. Using a rotatable feed through, samples can be positioned for either monochromator by simple rotation. The resolution of the energy analyzer ΔE_a (typically 0.1 to 0.4 eV) is determined by selecting the pass energy E_p ($=\Delta E_a R$), where the resolution $R \approx 125$.

The overall resolution of the instrument E_i is determined by taking the square root of the sum of the squares of photon plus electron contributions, i.e., $\Delta E_i = ((\Delta E_\lambda)^2 + (\Delta E_a)^2)^{1/2}$. ΔE_i could be as low as 0.15 eV at low photon energies (~30 eV), but for our results at higher photon energies (>50 eV) the minimum system resolution at which reasonable count rates could be achieved was 0.3 eV.

The spectra were all taken out on a recorder in analogue form with no multiscanning, although by varying time constants in the counting equipment we varied the effective count rate by a factor of 4. Full scans of both core d and valence band regions normally took about 25 min, while the d level scans took less than 10 min. A number of spectra of the d levels were usually recorded. The Sn 4d peaks, the In 4d peaks in $InCl_3$, and the Pb 5d peaks were digitized and computed to Lorentzian-Gaussian peak shapes using an iterative procedure described earlier.[11]

Table I. Compounds and Melting Points

Compd[a]	Mp, °C	Compd	Mp, °C
Ph_4Sn	226	$In(BzBz)_3$	251
$Cl_2Sn(BzAc)_2$	220	$In(AcAc)_3$	187
$Ph_2Sn(BzBz)_2$	240	$InCl_3$	586
$Me_2Sn(BzBz)_2$	190	$PbCl_2$	501
$Me_2Sn(BzAc)_2$	134-135	$Ga(AcAc)_3$	195
		Ph_4SbBr	210-214

[a] BzAc = anion of benzoylacetone; BzBz = anion of dibenzoylmethane; AcAc = anion of acetylacetone.

(B) **Compounds and Procedure.** The compounds used in this study are listed in Table I, along with their melting points. Some compounds were obtained commercially (Ph_4Sn, $InCl_3$, $PbCl_2$) or were prepared by well established methods.[12-14] All compounds readily sublime, and with the exception of $InCl_3$ all are stable to air and moisture. All the Sn compounds, $In(BzBz)_3$, $M(AcAc)_3$ (M = Ga, In), and Ph_4SbBr, are molecular unassociated compounds.[12-14] In contrast, both $InCl_3$ and $PbCl_2$ have highly associated structures. The In is surrounded by six Cl in an almost octahedral environment,[15] while the Pb has nine chlorine formally in the Pb coordinates environment at distances between 2.67 and 3.29 Å.[16]

For comparison with the spectra of solid Ph_4Sn, gas phase spectra of gaseous C_6H_6 were obtained at photon energies between 20 and 35 eV. The benzene was admitted to the reaction zone through a very fine nozzle.

For the solids, a few milligrams of compound were loaded into small Ta boats in the experimental chamber. At pressures in the 10^{-9} Torr region, the samples were heated in situ. With the exception of Ph_4SbBr, the compounds sublimed smoothly onto Pt, Au, or polished stainless steel substrates. A quartz crystal oscillator was used to monitor the amount of condensed compound. About 100 Å (±30 Å) of compound was sublimed onto the metal substrate. The thickness measurement is only semiquantitative because the evaporator-substrate-oscillator geometry was not accurately determined and it varied slightly for different sublimations. The thickness of the sample is quite critical. If too little compound is sublimed onto the substrate (~20 Å), then emission from the metal valence peaks still contributes to the spectrum, and relatively weak core d peaks are obtained. If, in contrast, the sample is too thick ($\geq$200 Å), the sample charges in the monochromatized beam, and the line widths broaden substantially. Indeed, if the sample is very thick ($\geq$1000 Å), the sample charges at a similar rate to the sweep rate of the spectrometer! For all our reported results in this paper, no observable charging occurred. Thus, the peaks did not shift noticeably ($\leq$0.1 eV) between successive spectra, and the distinct phenyl valence band peaks are within ±0.2 eV for all compounds containing the phenyl group.

The vapor pressure of most of the compounds is sufficiently small at room temperature so that very little sublimation occurred off the sample plate or crystal oscillator over a period of hours in a 10^{-9} Torr vacuum. However, $Me_2Sn(BzAc)_2$ and $In(AcAc)_3$ sublimed slowly from the substrate plate, and $Ga(AcAc)_3$ films sublimed in less than

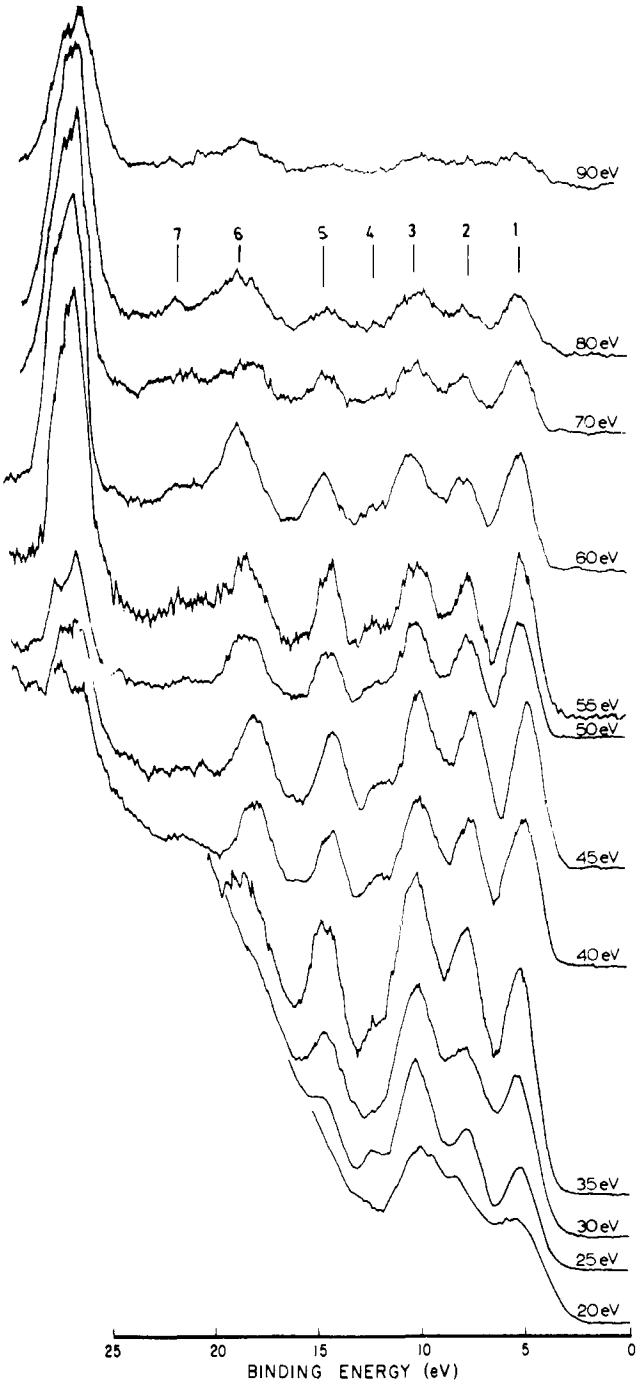

Figure 1. Low resolution spectra of evaporated Ph_4Sn films at different photon energies. The major valence band peaks are numbered above the 80 eV spectrum.

1 h. This made it difficult to obtain reproducible spectra for the latter compound.

There was no apparent problem with contamination of the sample surface despite the lack of ultra high vacuum conditions. The compounds do not apparently adsorb gases readily, and because most of the compounds are evaporating very slowly there is a "self-cleaning" effect operating.

For Sn and Pb metal, we have readily obtained the binding energies of the 4d and 5d lines respectively with respect to their Fermi edges. As discussed by Ley et al.,[7] the measurement of binding energies in insulators is a problem, especially in our present measurements where we do not have a strong sharp spectral feature in the backing material to reference against. In many cases we could see the Fermi edge of the backing Pt or Au, and we can then relate the binding energy (E_b) to the Fermi level of the sample:

$$E_B{}^F = h\nu - E_k - e\phi_s \quad (1)$$

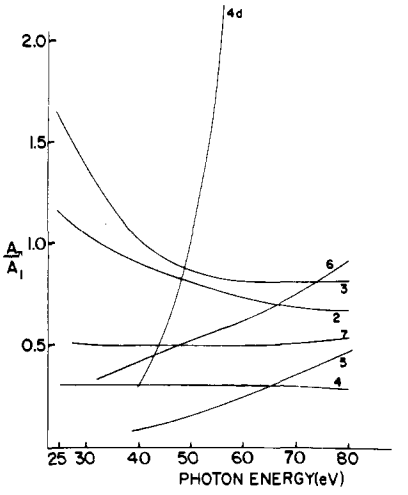

Figure 2. Relative cross sections of major peaks in the Ph_4Sn spectra [normalized to the low binding energy peak ($1e_{1g}$)] as a function of photon energy.

where $h\nu$ is the photon energy, E_k is the electron kinetic energy, and ϕ_s is the work function of the sample. Our binding energies still have only relative significance because of unknown work functions and very small charging shifts. However, several pieces of evidence suggest strongly that our *relative* binding energies are accurate to about ±0.2 eV. First, the phenyl valence band peaks all lie within ±0.2 eV. Second, our Sn 4d binding energies correlate well with previously obtained 3d binding energies (part III and Figure 9). Third, the differences in binding energy between previously obtained gas phase and our solid spectra are constant at 4.5 eV (part II, Tables II and III).

(II) Results and Discussion. Valence Bands

(A) Introduction. We wanted to be able to obtain both valence band spectra and core d level spectra of these compounds routinely at one photon energy. We first obtained spectra of Ph_4Sn at a range of photon energies at comparatively low instrumental resolutions (Figure 1). The instrumental resolutions corresponded very closely to one hundredth of the photon energy, i.e., 0.2 eV at 20 eV to 0.9 eV at 90 eV. A number of very general conclusions can be drawn from these preliminary spectra, and a plot of relative areas normalized to the low binding energy peak in the spectra (Figure 2). First, spectra, with adequate signal-to-noise ratio and uncontaminated by adsorbed gases, can be obtained readily without multiscanning. In fact, the signal-to-noise ratio improved after these initial spectra were recorded because the storage ring beam current increased by a factor of 2 to 3 before the later spectra were obtained. Second, the relatively narrow peaks (mostly due to the C_6H_5 groups) at constant binding energy indicate that charging effects are minimal for such samples. Third, the intensity of the Sn 4d peaks increases dramatically relative to the valence band peaks as the photon energy increases. Such increases in the 4d (and 5d) level cross sections above thresholds combined with decreases in p level cross sections (after an initial sharp increase) are well known.[17-19] Fourth, the secondary electron background rises very steeply at electron kinetic energies below 20 eV. To obtain adequate signal-to-noise ratios for *n*d ($n = 4, 5$) peaks, it appears to be essential that $h\nu \geq (E_b + 15)$ eV. This criterion will make it difficult to observe such core d peaks in insulating solids using He(II) radiation (40.8 eV). Fifth, the apparent resolution at low photon energies (20, 25 eV) is poorer than at middle to high photon energies, despite the better instrumental resolution at the lower energies. The reason for this is not entirely clear. The high secondary electron emission both obscures the peaks and apparently broadens the lines. Because the beam intensity is much greater at the low photon energies, it is also possible that we have some

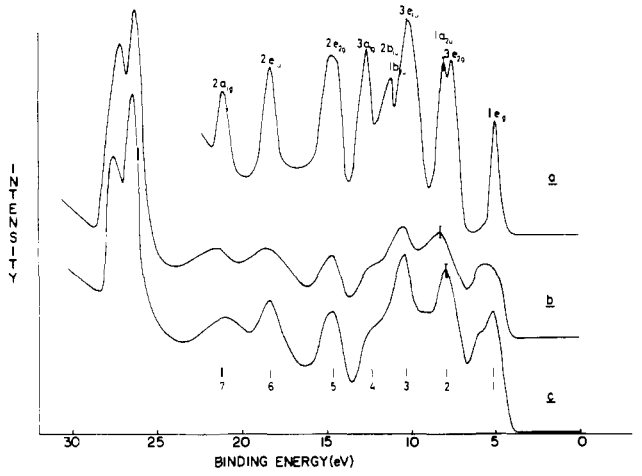

Figure 3. Photoelectron spectra of: (a) gaseous C_6H_6 taken with 30 eV photons and 0.35 eV instrumental resolution; (b and c) solid Ph_4Sn taken with 65 eV (b) and 57 eV (c) photons and 0.3 eV instrumental resolution. The statistical scatter in these and later spectra are indicated by the error bars which give the standard deviation of the count.

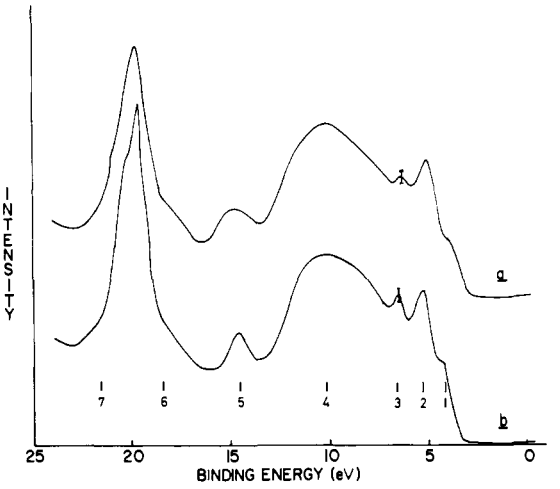

Figure 4. Photoelectron spectra of $In(AcAc)_3$ taken at 0.3 eV instrumental resolution and at photon energies of: (a) 48 eV; (b) 57 eV.

differential charge broadening. Finally, the decrease in quality of the spectra above 60 eV is due both to the decrease in synchrotron beam intensity and a decrease in monochromator efficiency at higher energies.

From these spectra, it is readily apparent that the optimum photon energy for obtaining well resolved Sn 4d peaks and valence bands of comparable intensity is between 50 and 60 eV. All the remainder of the spectra discussed in this work were recorded at photon energies between 45 and 65 eV.

(B) Valence Band Peaks. The photon energies used in this work enable the complete valence band spectra to be recorded, and the variable photon energy is sometimes useful for assignment purposes. Our data, combined with He(I) spectra on analogous gas phase compounds, enable us both to assign our spectra almost completely and to extend assignments from He(I) spectra. For example, He(I) spectra have been recorded in the gas phase for volatile acetylacetonates, and assignments have been made up to 18 eV binding energies (~13.5 eV in solids). We observe valence band peaks up to 22 eV binding energies in our solid acetylacetonates. Because most of our compounds contain phenyl and acetylacetonate groups, we first assign the Ph_4Sn and $In(AcAc)_3$ spectra (Figures 3 and 4).

In Figure 3, the spectra of solid Ph_4Sn at 57 eV and 65 eV photon energies are compared with a gas phase benzene spectrum which has been shifted by 4.5 eV so that the phenyl peaks in the two compounds closely coincide. For comparison purposes, the instrumental resolution for the benzene spectrum was deliberately chosen to be similar to the resolutions used for the Ph_4Sn spectra. The benzene spectrum is very similar to that given by Price using He(II) radiation,[21] and the peak positions (Table II) are in good agreement with literature values.[21,22] The assignment for the benzene spectrum (Table II) appears to be generally agreed on after animated debate[23-25] about the relative ordering of the $2b_{1u}$ and $3a_{1g}$ orbitals[24] and the $3e_{2g}$ and $1a_{2u}$ orbitals.[25]

The Ph_4Sn spectrum at 57 eV (Figure 3c) is very similar qualitatively to the benzene spectrum. The only marked additional feature in the Ph_4Sn spectrum is the shoulder at 5.7 eV binding energy. This shoulder increases in intensity markedly as the photon energy increases to 65 eV (Figure 3b). This change in intensity indicates that the 5.7 eV shoulder is not a component of a split $1e_{1g}$ benzene band as is often observed[1] in C_6H_5X compounds (X = electronegative substituent) but is due to the Sn-C bonding electrons. The good agreement between the valence band positions in C_6H_6 and Ph_4Sn (Table II) strongly suggests that we can interpret the Ph_4Sn spectrum in terms of a slightly perturbed C_6H_6 molecule and bonding Sn-C electrons (Table II). As indicated by the He(I) spectra of C_6H_5R compounds[1] (R = electropositive substituents, such as CH_3) it is not surprising that the replacement of H by Sn has very little effect on the benzene peaks.

Table II. Comparison of C_6H_6 and $(C_6H_5)_4Sn$ Valence Band Peak Positions (eV), ±0.1 eV

		C_6H_6		$(C_6H_5)_4Sn$
Band	and assignment	Lit.[a]	This work	This work
1	$1e_{1g}$	4.9	5.0	5.1
	t_2(Sn-C)			5.7
2	$3e_{2g}$	7.3	7.5	7.7
	$1a_{2u}$	7.7	7.9	
3	$3e_{1u}$	9.5		10.1
	$1b_{2u}$	10.3	10.1	
	$2b_{1u}$	10.9	11.1	
4	$3a_{1g}$	12.4	12.5	12.3
	a_1(Sn-C)?			
5	$2e_{2g}$	14.6	14.6	14.5
6	$2e_{1u}$	18.1	18.3	18.1
7	$2a_{1g}$	21.5	21.1	21.2

[a] Taken from ref 21 and 22 after subtracting 4.5 eV.

The assignment of the 5.7 eV peak to the t_2 Sn-C bonding molecular orbital is consistent with the gas phase Me_4Sn spectrum,[26] in which the t_2 (Sn-C) peak lies at 9.7 eV, i.e., 0.3 eV above the $1e_{1g}$ benzene peak in benzene. This difference is similar to the 0.6 eV observed for Ph_4Sn. Methyl and phenyl are known to be similar electropositive groups (or strong electron donors),[27] and their Sn-C MO's should be at similar energies. Using the Me_4M (M = Si, Ge, Pb) spectra[26] as a guide, it is likely that the a_1 component of the Sn-C bonding orbital lies about 6 eV above the t_2 orbital. The a_1 peak will probably still be rather weak at 50-60 eV photon energies and will be obscured by the $3a_{1g}$ benzene peak (band 4).

Returning now to Figure 2, it is apparent that peak 4 (due mainly to the benzene $3a_{1g}$ orgital, as well as Sn-C a_1 orbital) remains at the same relative intensity as the first band (largely due to the $1e_{1g}$ orbital, as well as the Sn-C t_2 orbital). This intensity information is consistent with assignment[22,24] of the 12.4 eV peak (16.9 eV in the gas phase) to the $3a_{1g}$ orbital of pure p character rather than to the $2b_{1u}$ having s character. Since both the Sn-C a_1 orbital and the $2b_{1u}$ orbital have large

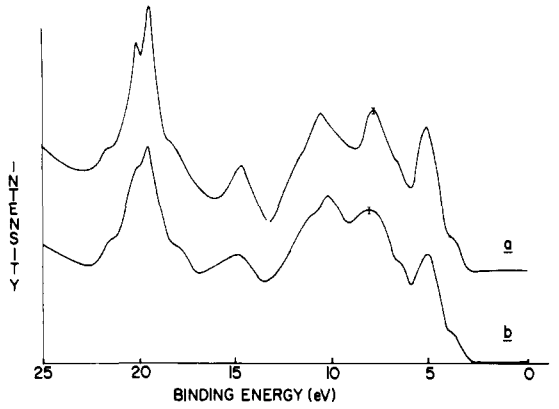

Figure 5. Photoelectron spectra of $In(BzBz)_3$ taken with: (a) 57 eV photons at 0.3 eV instrumental resolution; (b) 65 eV photons at 0.5 eV resolution.

Table III. Comparison of Gas Phase $Be(AcAc)_2$ and Solid State $In(AcAc)_3$ Valence Band Peak Positions (eV), ±0.1 eV

Band and assignment	$Be(AcAc)_2$[a]	$In(AcAc)_3$
1 π_3	3.9	4.1
2 n_-–p	5.2	5.2
3 n_+–p	6.6	6.5
4 C–C, C–H, π_2, π_1,?	8.5–11.5	8–12
5 C 2s		14.5
6 C 2s		~18.5 (±0.5)
7 C 2s		~21.5 (±0.5)

[a] Taken from ref 20 after subtracting 4.5 eV from the He(I) gas phase data.

s characters, the intensity of band 4 would be expected to increase substantially with photon energy relative to band 1 with the latter assignment. Peaks 5, 6, and 7 increase in intensity substantially, as expected for MO's having large C s characters.

The $In(AcAc)_3$ and $Ga(AcAc)_3$ spectra are qualitatively similar to each other, although the Ga 3d peaks are substantially less intense than the In 4d peaks. $Ga(AcAc)_3$ sublimed too rapidly to obtain reproducible spectra, and we do not report the $Ga(AcAc)_3$ spectra here. Up to ~13 eV on our binding energy scale (~18 eV for gas phase compounds), the $In(AcAc)_3$ spectrum is very similar qualitatively to the gas phase spectra of $Be(AcAc)_2$ and non-transition-metal hexafluoroacetylacetonate's taken previously by Evans et al. using He(I) radiation.[20] Our interpretation follows theirs for the low-energy peaks.

From simple Hückel theory, the π system of the six-membered M(AcAc) ring results in five MO's, with orbital energies $\pi_1 < \pi_2 < \pi_3 < \pi_4 < \pi_5$.[28] π_3 is involved in bonding, while π_1 and π_2 lie substantially below π_3 (~5 eV) and π_4 and π_5 substantially above π_3. Mass spectral appearance potential data[29,30] first suggested that π_3 was the filled orbital of highest energy in many metal complexes, and the photoelectron spectra confirmed this interpretation.[20] For σ bonding the symmetric and antisymmetric combination of the in-plane O_{p_x} orbitals on the acetylacetonates give rise to n_+ (a_1) and n_- (b_1) orbitals, respectively, which can interact with the 5s and 5p orbitals on the In or Sn. The ordering of ligand orbitals is thought to be $n_+ < n_- < \pi_3$.[20] The major source of metal–ligand bonding is expected to be the n_+–p and n_+–s interactions. The D_3 point group of these tris chelates will cause a splitting of all bands into e and a components, but this splitting is usually not resolved. Evans et al.[20] assigned the first three bands generally observed in non-transition-metal acetylacetonates and in $Be(AcAc)_2$ as given in Table III. The excellent agreement

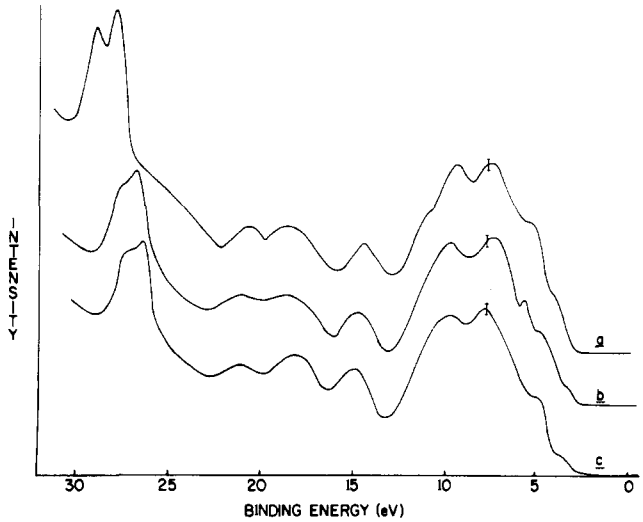

Figure 6. Photoelectron spectra of Sn compounds taken at 57 eV photon energy: (a) $Cl_2Sn(BzAc)_2$ (b) $Me_2Sn(BzBz)_2$ taken at 0.43 eV instrumental resolution; (c) $Me_2Sn(BzBz)_2$ taken at 0.43 eV instrumental resolution.

Table IV. Valence Band Peak Positions (eV) for $In(BzBz)_3$, $Me_2Sn(BzAc)_2$, $Me_2Sn(BzBz)_2$, and $Cl_2Sn(BzAc)_2$,[a] ±0.1 eV

$In(BzBz)_3$	Me_2Sn-$(BzAc)_2$	Me_2Sn-$(BzBz)_2$	Assignment
4.0	3.6	3.7	π_3
5.2	4.8	5.0	$1e_{1g}$ n_-–5p (Sn–C)
6.5	5.6 (±0.3)	Not resolved	n_+–5p (Sn–C)?
7.8	7.2	7.3	$3e_{2g}$ $1a_{2u}$
10.6	9.8	9.3	$3e_{1u}$, $1b_{2u}$, $2b_{1u}$ C–C, C–H, π_2, π_1
14.8	14.6	14.1	$2e_{2g}$ + C 2s of AcAc
18.5 (±0.5)	18.0	18.0	$2e_{1u}$ + C 2s of AcAc
21.5 (±0.5)	20.8	20.5	$2a_{1g}$ + C 2s of AcAc

[a] All the valence band peaks for $Cl_2Sn(BzAc)_2$ are within 0.3 eV of the $Me_2Sn(BzBz)_2$ peaks except for the first peak at 4.4 eV (which is assigned to π_3 + nonbonding Cl electrons).

between the $In(AcAc)_3$ and "normalized" $Be(AcAc)_2$ results strongly suggests that the same assignment is appropriate for $In(AcAc)_3$. The broad band from 8 to 12 eV arises from ionizations of the C–H and C–C bonding electrons, as well as the acetylacetonate π_2 and π_1 bands. The three peaks at higher energies (14.5, 18.5, and 21.5 eV) are at very similar energies to the (mainly) C 2s peaks in benzene (Table II) and are at similar energies to the C 2s peaks in C_3H_8.[31] It seems reasonable then to assign these peaks to MO's of high C 2s character from the three ring carbons in $In(AcAc)_3$. The O 2s peaks[32] may also contribute to the high-energy shoulder of the In 4d peak at about 21.5 eV.

The spectra of $In(BzBz)_3$, $Me_2Sn(BzAc)_2$, $Me_2Sn(BzBz)_2$, and $Cl_2Sn(BzAc)_2$ (Figures 5 and 6, Table IV) have features common to both the Ph_4Sn and $In(AcAc)_3$ spectra, and most assignments can be readily made by direct comparison of peak positions (Tables III and IV). In $In(BzBz)_3$, the first two peaks in the spectra at 4.0 and 5.2 eV are both due to π MO's, π_3 from the acetylacetone ring and $1e_{1g}$ from the C_6H_5 ring, respectively. Here we have the rather interesting case of two nonbonding π orbitals lying at lower binding energies than bonding σ orbitals. The n_- orbital peak is superimposed on the

Table V. Peak Parameters for 4d (and 5d) Levels for Sn, In, Sb, and Pb Compounds

Compd[a]	No. of spectra	Instrumental resolution, eV	Binding energies[b] eV	Widths,[c] eV	SO splitting,[d] eV	Intensity ratio[d]
Sn metal	6	0.30	23.95 } $E_f = 0$	0.56 (1)	1.05 (1)	1.33 (3)
			25.00 }	0.65 (1)		
Ph_4Sn	12	0.30	25.69	0.71 (1)	1.04 (1)	1.38 (6)
			26.73	0.82 (1)		
	3	0.43		0.79 (2)		
				0.90 (2)		
	2	0.64		0.99 (3)		
	2	0.90		1.09 (5)		
$Cl_2Sn(BzAc)_2$	3	0.30	27.07	0.87 (3)	1.07 (2)	1.51 (10)
			28.14			
	7	0.43		0.96 (4)		
$Ph_2Sn(BzBz)_2$	7	0.30	26.23	0.97 (4)	1.06 (1)	1.34 (10)
			27.29			
	5	0.43		1.01 (4)		
	3	0.72		1.24 (5)		
$Me_2Sn(BzBz)_2$	3	0.30	26.20	0.96 (4)	1.06 (1)	1.5 (1)
			27.26			
	7	0.43		1.05 (5)		
$Me_2Sn(BzAc)_2$	2	0.30	26.34	1.06 (4)	1.05 (1)	1.5 (1)
			27.39			
	3	0.43		1.07 (5)		
$InCl_3$	2	0.30	19.48	0.95 (4)	0.88 (4)	1.86 (10)
			20.36			
$In(BzBz)_3$	4	0.30	19.8	~0.8	~0.8	Not computed
			20.6			
$In(AcAc)_3$	4	0.30	19.8	~0.9	~0.8	Not computed
			20.6			
Pb metal	4	0.37	17.93 } $E_f = 0$	0.65 (1)	2.63 (1)	Ref 68
			20.56 }			
$PbCl_2$[e]	4	0.30	20.12	0.73 (1)	2.61 (1)	1.37 (2)
			22.73	0.73 (1)		
Ph_4SbCl	2	0.43	34.88	1.01 (5)	1.24 (3)	1.46 (5)
			36.12			

[a] BzAc, anion of benzoylacetone; BzBz, anion of dibenzoylmethane; AcAc, anion of acetylacetone. [b] Taken from evaporations onto Pt metal. Reproducibility is better than 0.1 eV. [c] Taken from all evaporations onto Pt and stainless steel. Whenever the widths of the $d_{3/2}$ and $d_{5/2}$ peaks are significantly different, both widths are given; otherwise, the average of the two is given. Standard deviations (external) are given in parentheses. [d] Standard deviations are given in parentheses. [e] Binding energy with respect to the vacuum level ~24.6 eV (G. M. Bancroft, D. E. Eastman, and W. Gudat, to be published).

$1e_{1g}$ phenyl peak, while the n_+ peak is readily seen at 6.5 eV. The remainder of the spectrum is very similar to both the Ph_4Sn and $In(AcAc)_3$ spectra, although the peaks overlapping the In 4d peaks at ~18.5 and 21.5 eV are substantially stronger in $In(BzBz)_3$ than in $In(AcAc)_3$ due to the six phenyl groups in $In(BzBz)_3$.

The low binding energy peak in the Me_2Sn compounds and $Cl_2Sn(BzAc)_2$ (Figure 6) can also be assigned to the π_3 electrons. The peaks at 3.6–3.7 eV in the Me_2Sn compounds and 4.4 eV in $Cl_2Sn(BzAc)_2$ lie at significantly lower and higher binding energies, respectively, than in $In(BzBz)_3$. These shifts could be due to increased π bonding between the metal and AcAc ring in the order $Cl_2Sn(BzAc)_2 < In(BzBz)_3 < Me_2Sn$ compounds and/or a straightforward chemical shift effect. It is interesting that the Sn 3d and 4d binding energies (Table V, Figure 9) increase by about the same amount as the π_3 energies on going from Me_2Sn compounds to $Cl_2Sn(BzAc)_2$. Features due to nonbonding Cl electrons, Cl 3s electrons, or Sn–Y (Y = Me, Cl) bonding electrons could not be detected positively in these three compounds.

The structure of $InCl_3$ in the solid state consists of In surrounded by six chlorines in a near octahedral environment.[15,16] The spectrum (Figure 7) can be interpreted on the basis of the simple molecular orbital diagram for MX_6 complexes[33] combined with gas phase data on chlorine containing compounds such as CCl_4[2a] and SiH_3Cl.[34] A partial valence band for the similar $SnCl_6^{2-}$ species has also been published,[35] and

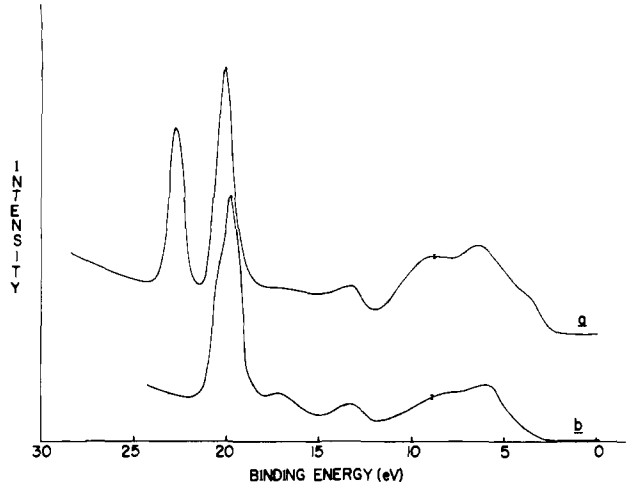

Figure 7. Photoelectron spectra of: (a) $PbCl_2$ taken with 65 eV photons at 0.5 eV instrumental resolution; (b) $InCl_3$ taken with 57 eV photons at 0.3 eV instrumental resolution.

the first two peaks in $InCl_3$ and $SnCl_6^{2-}$ are at similar positions. However, the previous interpretation of the $SnCl_6^{2-}$ spectrum appears to be incomplete. The lowest binding energy peak in $InCl_3$ centered at ~6 eV is due to the 12 Cl p_π electrons which are the t_{1g}, t_{2g}, $3t_{1u}$, and t_{2u} MO's of an octahedral

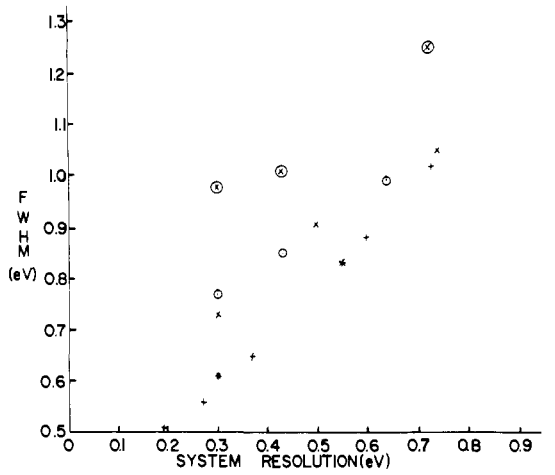

Figure 8. Full width at half-maximum for Sn 4d and Pb 5d peaks plotted vs. the instrumental resolution for: $Ph_2Sn(BzBz)_2$ (⊗); Ph_4Sn (⊙); $PbCl_2$ (×); Pb metal (+); Sn metal (*). The Sn metal value at 0.55 eV system resolution was taken from ref 69.

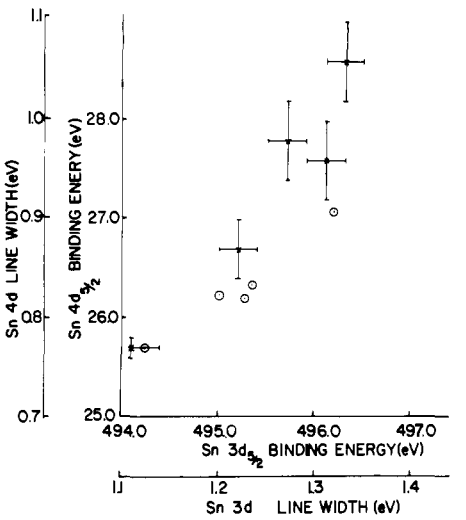

Figure 9. Correlation of Sn 3d binding energies and fwhm (ref 8) with Sn 4d binding energies and fwhm in this paper.

complex. The peak centered at about 8 eV is mostly due to the $2t_{1u}$ orbital, the Cl_{3p}–In_{5p} bonding orbital. The next peak at ~14 eV can be attributed to the $2a_{1g}$, $2e_g$ orbitals of mainly Cl_{3p}–In_{5s} character. The peak at about 17.5 eV can be attributed to the Cl_{3s} orbitals, the $1a_{1g}$, $1t_{1u}$, and $1e_g$ octahedral MO's.

The $PbCl_2$ spectrum is qualitatively similar, although the low binding energy region shows three broad bands compared to two in $InCl_3$. The structure of $PbCl_2$ is highly distorted[16] and no detailed interpretation can be made. However, the distorted Pb coordination environment will split many of the degenerate octahedral MO's discussed for $InCl_3$. It is not unreasonable then that $PbCl_2$ has an additional band and broader peaks than $InCl_3$.

The Cl 3s peak, especially in the $PbCl_2$ case, is very weak in these spectra. At higher photon energies (≥70 eV), the Cl 3s peak(s) (at about 17 eV) became more intense in $PbCl_2$. The Cl 3s cross section is known to be very small relative to metal d peaks at these low photon energies.[17,36] Indeed, the ionization from the Cl 3s orbitals in gaseous mercuric chloride has not been seen[17] because of the very low cross section at 40.8 eV (He(II)) photon energy.

(III) Results and Discussion. Core d Levels

(A) Line Widths and Chemical Shifts. With the exception of $In(AcAc)_3$ and $In(BzBz)_3$, the computed peak parameters are given in Table V. Because carbon valence band peaks overlap the In 4d peaks of these compounds (Figures 4 and 5), it was impractical to compute these spectra. Spectra were obtained at 0.3 eV system resolutions for all compounds and sometimes at other resolutions (Table V, Figure 8). The Pb 5d line widths for Pb metal, $PbCl_2$, and other lead compounds are given in more detail elsewhere.[37]

When Pt metal was used as the substrate, Sn 4d peak positions usually occurred at slightly lower binding energies (~0.5 eV) than with stainless steel substrates. Binding energies in Table V are quoted for Pt substrates. *Relative* binding energies, however, were not affected by the substrate. With the exception of $Me_2Sn(BzBz)_2$ and $Cl_2Sn(BzAc)_2$, widths of the 4d peaks did not differ noticeably between the two substrates.

With the exception of Sn metal and Ph_4Sn, the component $d_{3/2}$ and $d_{5/2}$ line widths are equal within the experimental error. As a result, we usually quote the average widths in Table V. For other compounds, such as $Ph_2Sn(BzBz)_2$, the $d_{5/2}$ line width (0.93 ± 0.05 eV) tended to be smaller than the $d_{3/2}$ line width (1.00 ± 0.05 eV). The widths quoted in Table V for Ph_4Sn and $Ph_2Sn(BzBz)_2$ are in agreement with the preliminary results,[9] while the width for $Me_2Sn(BzBz)_2$ is appreciably smaller (~0.1 eV) than that quoted previously. The narrower widths quoted here refer to stainless steel substrates, rather than the Pt substrates used earlier.

The 4d Sn metal spectrum has been published recently,[38] and the difference in $4d_{3/2}$ and $4d_{5/2}$ widths quoted in Table V has been explained using many body effects[39] which lead to asymmetries on the high binding energy side of metal lines. When symmetric line shapes are fitted to these asymmetric lines, the $4d_{3/2}$ line artificially broadens to compensate for these asymmetries. The difference in Ph_4Sn line widths is not readily rationalized at the present time. It cannot be due to ligand field effects which if anything broaden the $d_{5/2}$ line relative to the $d_{3/2}$ line in such a tetrahedral molecule.[40]

As commented on in a previous paper,[41] the cleanliness of the metal surface does not appear to be the ultimate factor in obtaining narrow core lines in solids. For example, evaporation onto clean in situ Au surfaces[41] gave broader lines than those obtained by evaporation onto "dirty" Pt. The present work shows that lines on oxide-contaminated stainless steel are at least as narrow as those on Pt. These results suggest that different layers of nonconductor on a very clean metal surface may have different chemical shifts, and line broadening then occurs.

As predicted in our initial study of Sn 3d line widths,[8] the insulator line widths have decreased greatly with decrease in source line width. Thus the molecular Ph_4Sn and ionic $PbCl_2$ both give line widths within 0.15 eV of metal line width, and it is apparent from the plot in Figure 8 that these line widths will decrease substantially more with a decrease in instrumental resolution. Thus the slopes of the line in Figure 8 for $PbCl_2$ and Pb metal are 0.72 and 0.87, respectively, and the extrapolated inherent line widths (to zero system resolution) for $PbCl_2$ and Pb metal are 0.53 and 0.34 eV, respectively.[37] These narrow insulator line widths are especially pleasing because the charging possibilities (and the associated differential charge broadening) are so much greater in this study with monochromatized synchrotron radiation than with our nonmonochromatized McPherson instrument.

The correlations given in Figure 9 again indicate that we have virtually eliminated charging effects in both nonmonochromatized (Sn 3d) and monochromatized (Sn 4d) studies. Thus there is a good correlation between Sn 4d and Sn 3d binding energies. To first order, different core lines should be equally sensitive to chemical effects.[42] A slope of slightly less than one observed in Figure 9 is not unreasonable considering

Table VI. Measured Nuclear Quadrupole Splittings and 3d and 4d Line Widths for Solid Sn Compounds

Compd	$\frac{1}{2}e^2Qq$,[a] mm S^{-1}	3d line width,[b] eV	4d line width,[c] eV
Ph_4Sn	0	1.11	0.77
$Cl_2Sn(BzAc)_2$	~0.6	1.22	0.87
$Ph_2Sn(BzBz)_2$	2.15	1.27	0.97
$Me_2Sn(BzBz)_2$	4.08	1.31	0.96
$Me_2Sn(BzAc)_2$	3.87	1.33	1.06

[a] Reference 12. [b] Reference 8. [c] Table V, this work, at 0.3 eV resolution.

the errors of ±0.1 eV and possible second-order shifts[42-44] which should lead to a smaller chemical shift for the outer $n = 4$ level,[2b] as observed. There is also a correlation of 4d line width (Figure 9) and 3d line width, and the slope of the correlation is appreciably greater than one.

(B) Ligand Field Broadening and Splitting of d Peaks. The line width correlation in Figure 9 shows that the 3d and 4d Sn line widths increase concurrently. The data in Table VI and in Figure 10 show that there is a correlation between 3d and 4d line widths and the ^{119}Sn nuclear quadrupole splittings as measured by Mössbauer spectroscopy. The broadening effect is seen in Figure 10, in which the 4d spectra are shown in order of increasing electric field gradient measured at the nucleus. A well-resolved 4d doublet in Sn metal, Ph_4Sn, and $Cl_2Sn(BzAc)_2$ degrades into a very poorly resolved doublet in the two Me_2Sn compounds (Figure 10e,f). Using the preliminary results on Ph_4Sn and $Ph_2Sn(BzBz)_2$, combined with the high resolution spectrum of the Cd 4d levels in Me_2Cd,[9] we have presented[9] convincing evidence that the *trend* in Sn d widths and the splitting in the 4d levels in Me_2Cd is due to ligand field splitting of the $4d^9$ state produced in the photoelectron experiment. In particular, the splitting is due to the so called asymmetry or field gradient C_2^0 term[45,46] in the crystal field expansion. The present, more extensive, Sn 4d data further support our interpretations, and recent calculated[47] and observed[48] ligand field splittings in XeF_2 and XeF_4 confirm our approach. Because of the considerable generality of this ligand field effect[45,46] for splitting and broadening of core $p_{3/2}$, d, and f levels in photoelectron spectra, we present the underlying theory in some detail before examining the Sn, Cd, and Xe 4d data. We then correlate the derived C_2^0 values with the known electric field gradients measured at the nuclei. Finally, we comment on the possible magnitude of other broadening mechanisms, which we have indicated are unimportant[8,9] in producing the overall trend in line widths.

We assume that there is no bonding between the 4d levels and the ligands. For the Sn 4d levels with binding energies ≥25 eV (relative to the Fermi level), this assumption is reasonable. Moreover, the similar chemical shifts for the 4d and 3d levels (Figure 8) strongly suggest that the 4d levels are corelike. Even for the Cd 4d levels in Me_2Cd ($E_b \approx 17$ eV), the spectrum is consistent with a crystal field effect rather than bonding. For our six-coordinate Sn compounds, the effective symmetry[40] of both cis and trans complexes is D_{4h}, so that the required crystal field potential is:[40]

$$V = B_2^0(3z^2 - r^2) + B_4^0(35z^4 - 30r^2z^2 + 3r^4) + B_4^4(x^4 - 6x^2y^2 + y^4) \quad (2)$$

For tetrahedral Ph_4Sn, the B_2^0 term is not present in the potential expansion. Including the spin-orbit coupling, our Hamiltonian becomes:

$$\mathcal{H} = V + \lambda LS \quad (3)$$

This Hamiltonian interacts with the d^9 state produced in the photoelectron experiment. The ligand field states for a d^1 (or d^9) ion arise from the ^2D term of the free ion, so the ten functions $L = 2, M_L; S = \frac{1}{2}, -\frac{1}{2}$ form a convenient basis set. Using the method of operator equivalents[49] the Hamiltonian of eq 3 can be rewritten in the form:

$$\mathcal{H} = C_2^0[3L_z^2 - L(L+1)] + C_4^0[35L_z^4 - 30L(L+1)L_z^2 + 25L_z^2 - 6L(L+1) + 3L^2(L+1)^2] + C_4^4(L_+^4 + L_-^4) + \lambda[\tfrac{1}{2}(L_+S_- + L_-S_+) + L_zS_z] \quad (4)$$

where $L = 2, S = \frac{1}{2}$; L_z, $L_\pm$, and $S_\pm$ are the usual orbital and spin angular momentum operators. All present theoretical and experimental evidence indicates that the C_4 terms are much smaller than the asymmetry or field gradient C_2^0 term. Thus Ph_4Sn (with no C_2^0 term) gives the narrowest line widths, while the well-resolved Me_2Cd and XeF_2 spectra can be fitted with just C_2^0 terms. In addition, present theoretical evidence[47,50] suggests that the C_2^0 term is at least an order of magnitude larger than the C_4^0 term. Thus, if we assume that the Me_2Sn linkage sets up a large fraction of the crystal field,[51] a simple crystal field calculation[50] shows that $C_2^0/C_4^0 = 3a^2/r^2$, where a = the Sn–Me distance (~2.2 Å)[51] and r = the effective radius of the Sn 4d electrons (~0.5 Å).[52] It is thus reasonable to neglect the C_4 terms, and our Hamiltonian becomes:

$$\mathcal{H} = C_2^0[3L_z^2 - L(L+1)] + \lambda[\tfrac{1}{2}(L_+S_- + L_-S_+) + L_zS_z] \quad (5)$$

The symmetric 10 × 10 Hamiltonian matrix is readily reduced to a 5 × 5 matrix, and after diagonalizing, the following five energy levels result.

$$E_1 = 6C_2^0 + \lambda \quad (6a)$$

$$E_{2,3} = \tfrac{3}{2}C_2^0 - \tfrac{1}{4}\lambda \pm \frac{(81C_2^{0^2} - 27C_2^0\lambda + \frac{25}{4}\lambda^2)^{1/2}}{2} \quad (6b)$$

$$E_{4,5} = -\tfrac{9}{2}C_2^0 - \tfrac{1}{4}\lambda \pm \frac{(9C_2^{0^2} - 3C_2^0\lambda + \frac{25}{4}\lambda^2)^{1/2}}{2} \quad (6c)$$

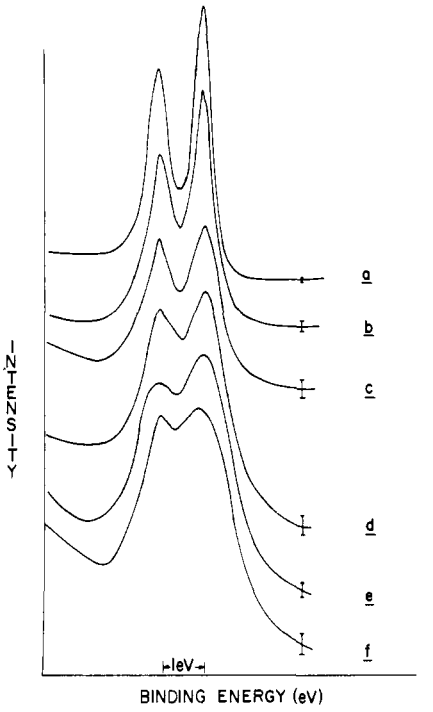

Figure 10. Typical Sn 4d spectra (recording time ~10 min) of Sn metal and solid nonconductor Sn organometallic thin films taken at 0.3 eV instrumental resolution at a photon energy of 57 eV: (a) Sn metal; (b) Ph_4Sn; (c) $Cl_2Sn(BzBz)_2$; (d) $Ph_2Sn(BzBz)_2$; (e) $Me_2Sn(BzBz)_2$; and (f) $Me_2Sn(BzAc)_2$. The spectra are drawn one under the other for convenience. The binding energies are given in Table V.

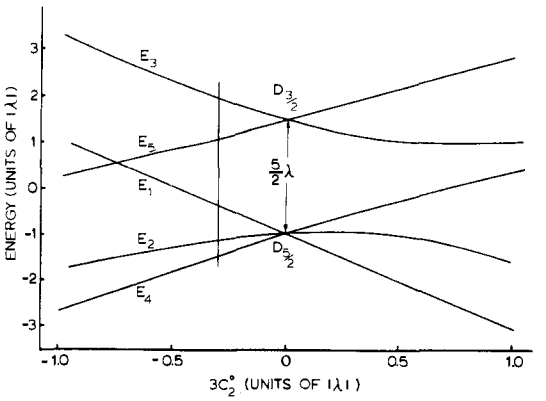

Figure 11. Energy level diagram for the combined spin-orbit coupling and electric field gradient interaction. The energy levels are numbered as in eq 6. The line indicates the $3C_2^0$ value for the Me_2Sn compounds.

For the d^9 case, we change the sign of λ[40] and C_2^0 and then set $3C_2^0$ equal to different fractions of λ. The energy level diagram in Figure 11 results. This is similar in form to that given by Ley et al.[53]

The crystal field part of the Hamiltonian in eq 5 transforms like the nuclear electric quadrupole interaction, neglecting the η (or C_2^2) term.[54]

$$\mathcal{H} = \frac{e^2qQ}{4I(2I-1)}[3I_z^2 - I(I+1)] \qquad (7)$$

where I and I_z are the nuclear spin and nuclear spin momentum operators, respectively; eQ is the quadrupole moment of the nucleus; and eq is the electric field gradient (EFG) set up by the ligands. C_2^0 is thus proportional to q, and the splitting (or broadening) at the electronic sites should be proportional to the EFG splitting at the nucleus, as is seen in Table VI and Figure 10 for our tin compounds.

It is important to emphasize that for the crystal field interaction a negative C_2^0 term results when the stronger field ligands lie along the Z EFG axis, as in *trans*-$Me_2Sn(BzBz)_2$. Conversely, if the in-plane ligands exert a stronger field than the axial ligands, as in *cis*-$Ph_2Sn(BzBz)_2$, the C_2^0 term will be positive. It is well known that the ratio of trans:cis field gradients is $2:-1$[54] and this kind of structural difference in EFG's is very useful for structure and bonding studies in inorganic chemistry.

The energy level diagram in Figure 11 shows that at our resolutions, a broadening of the spin-orbit doublet will occur for positive and negative C_2^0 up to about $3C_2^0 = 0.3|\lambda|$ ($C_2^0 \sim 0.04$ eV). At larger C_2^0 values, the doublet feature will be lost, and at large positive C_2^0 values, a triplet structure could appear. To obtain an average estimate for the C_2^0 term in $Me_2Sn(BzAc)_2$ and $Me_2Sn(BzBz)_2$, we calculate the difference in line width between the analogous six-coordinate Me_2Sn and Cl_2Sn compounds at both 0.3 and 0.43 eV resolutions. The average difference in widths is 0.12 ± 0.03 eV. This leads to a $d_{3/2}$ splitting of 0.31 ± 0.05 eV and a C_2^0 value of -0.036 ± 0.006 eV. These values are slightly larger than those for Me_2Cd, as expected from the relative nuclear field gradients (Table VII).

Recently, we became aware of the absorption studies on XeF_2 and XeF_4,[48] which showed clear evidence for ligand field splitting of the Xe 4d levels. The consistency between these results and ours is important to comment on here, because it further confirms the nature and magnitude of the Sn 4d splittings. The Hamiltonian matrix in this paper is identical in form to that given by Comes[48] and Basch.[47] They also neglected the C_4^0 term, but Comes used two asymmetry parameters δ and δ' to fit their spectra. However, δ is not significantly different from δ', and their matrix reduces to ours when $3C_2^0 = \delta\ (=\delta')$ and when their λ is replaced by $\frac{5}{2}\lambda$. Using the molecular orbital calculations as a guide in fitting their spectra, Comes obtained C_2^0 values (taking $6C_2^0 = \delta + \delta'$) in the 0.04 eV range (Table VII) compared to the values calculated by Basch in the 0.06 eV range. Errors in the derived parameters were not given, but Schwarz (private communication) estimates the reliability of his results at ±20%.

Table VII. Electric Field Gradients (EFG) at Nuclei and 4d Electronic Sites in Cd, Sn, and Xe Compounds

Compd	EFG at nucleus, $\lvert eq\rvert$, esu cm^{-3}	Ref	$\lvert C_2^0\rvert$(4d), eV	Ref
Me_2Cd	2.6×10^{16}	9	0.026 (0.001)	9
$Me_2Sn(BzBz)_2$	3.4×10^{16}	9	0.036 (0.01)	This work
XeF_2	8.4×10^{16}	55	~0.042 (obsd)	48
			0.061 (calcd)	47
XeF_4	8.8×10^{16}	55	~0.043 (obsd	48
			0.065 (calcd)	47

It is apparent (Table VII) that the C_2^0 values for XeF_2 and XeF_4 are, if anything, larger than those for Me_2Cd and the Me_2Sn compounds, as expected qualitatively from the larger electric field gradients at the Xe nucleus measured by Mössbauer spectroscopy.[55] Quantitatively, the C_2^0 values for XeF_2 and XeF_4 are considerably smaller than expected from the relative nuclear field gradients (Table VII). The detailed theory for such d splittings in terms of the so-called quadrupole overlap parameters, $\langle F^2\rangle$,[56,57] has not yet been worked out for these elements, and good MO calculations are only available for the Xe fluorides. Clearly, however, we would expect the Xe 4d splitting to be smaller than expected from the nuclear field gradients because the Xe 4d binding energies are considerably larger (~50 eV) than the Cd or Sn 4d binding energies, and it is known that the ligand field splitting decreases with increase in binding energy.[47,56]

ESCA studies of xenon fluorides[2b,59] have examined chemical shift differences between Xe gas and the fluorides, but there has been no attempt to look at the 3d or 4d widths. Indeed, Carroll et al.[59] dismissed any ligand field broadening of the 3d levels as being negligible, without quoting any widths. In fact, Basch's calculations[47] show that the splitting of the 3d levels should be close to one-half that of the 4d levels, and such a splitting would lead to about a 0.05–0.1 eV broadening of the 3d levels in XeF_2 relative to Xe. Such a broadening is just of the order observed by us for the Sn 3d levels. Gupta and Sen's calculations[56,57] also show that the splitting of core levels, for example in Tm compounds, decreases rather slowly from outer to deeper core levels. A careful high resolution ESCA study of the Xe 3d and 4d line widths in XeF_2 and XeF_4 would now seem to be very desirable and is now underway.[48b]

Finally, we comment on the role of other possible broadening mechanisms. It is apparent from Table VI that our correlation of 3d and 4d line widths with nuclear quadrupole splitting is not perfect; in particular the Ph_4Sn line widths are appreciably narrower (≥0.1 eV) than the $Cl_2Sn(BzAc)_2$ line widths, whereas, the two line widths should be very similar from their very small nuclear quadrupole splittings (Table VI). This difference could be due to the greater radiation stability of Ph $_4$Sn. Because of the above difference, we have considered just the analogous six-coordinate Cl_2Sn, Ph_2Sn, and Me_2Sn compounds in deriving our C_2^0 term for the Me_2Sn compounds. Within this six-coordinate series, other broadening mechanisms cannot explain the *trend* in line widths. Vibrational broadening[60] will not be an important contributing factor to the line widths in these heavy molecules. All vibrational frequencies in these molecules[12] are less than 0.08 eV, and Cd,[9] Zn,[62] and Hg[63] molecules having similar vibrational frequencies give little (<0.1 eV) broadening even at 0.05 eV

resolutions. At our present resolution, such an effect would broaden the line by ≤0.02 eV. Moreover, the *variation* in vibrational broadening in the six-coordinate analogues will be much less than 0.02 eV. Phonon broadening[64,65] (due to intermolecular vibrations) can also be an important broadening contribution, but it is not possible yet to calculate this contribution in molecular solids. However, our very similar Sn 3d line widths[8] for gases and solids show that this broadening is no larger than ~0.1 eV in these compounds. Once again, the *variation* in phonon broadening in the six-coordinate analogues must be much less than this value. The Auger broadening mechanisms[66] have only been well documented for the C and F 1s levels[66] and S 2s level.[44] For our compounds, there is no reasonable correlation of line widths with chemical shifts, as expected if these mechanisms are important. For example, the expected trend of a decrease in line width with increase in binding energy[66] is not present.

The evidence given above for the phonon and Auger broadening mechanisms is, of course, not conclusive by itself. However, the consistency of the C_2^0 values for Cd, Sn, and Xe compounds seems to be indisputable evidence that the *major* contribution to the increase in 4d and 3d widths is due to the ligand field splitting.

(C) Spin-Orbit Splittings and the $d_{5/2}$:$d_{3/2}$ Ratio. All Sn compounds give spin-orbit splittings of 1.05 ± 0.02 eV. Similarly, our spin-orbit splittings for In, Sb, and Pb compounds are in excellent agreement with previous literature values[53,67] and with free atom values. Our results, on compounds having ligands of widely varying bonding properties, strongly suggest that the spin-orbit splitting is not dependent on the chemical environment. In particular, the apparent spin-orbit splitting does not increase noticeably with an increase in the C_2^0 term. We showed previously[9] that the increase in apparent spin-orbit splitting in Cd metal cannot be due to the C_2^0 term as proposed by Ley et al.[53]

Although the errors in the peak heights are generally large (Table V), the ratio of intensity of the $d_{5/2}$:$d_{3/2}$ peaks varies substantially from one compound to another. For example, the ratio in $InCl_3$ is much larger than in Sn metal or Ph_4Sn. These results strongly suggest that this ratio is chemically sensitive, and a subsequent paper examines in detail this ratio in the 5d peaks of Pb compounds.[68]

Acknowledgments. We are very grateful for the outstanding assistance of Dr. E. Rowe and the technical staff at the Physical Sciences Laboratory, Stoughton, Wisconsin, and the assistance of Dr. I. Adams in the preliminary stages of this work. G.M.B. wishes to acknowledge with gratitude the award of the Canadian E.W. Steacie Fellowship (1973-1976) which made it possible to do this work. The financial assistance of NRC (Canada) and the NSF (Grant No. DMR-74-15090) is acknowledged.

References and Notes

(1) (a) University of Western Ontario; (b) IBM Thomas J. Watson Research Center.
(2) (a) D. W. Turner, A. D. Baker, C. Baker, and C. R. Brundle, "Molecular Photoelectron Spectroscopy", Wiley, New York, N.Y., 1970; (b) K. Siegbahn et al., "ESCA-Atomic, Molecular and Solid State Structure by means of Electron Spectroscopy", Series IV, Vol. 20, Nova Acta Regiae Soc. Sci. Upaliensis, Uppsala, Sweden, 1967.
(3) For example, see the recent papers using monochromatized Al Kα radiation as the source and instrumental resolutions of about 0.3 eV. U. Gelius, E. Basilier, S. Svensson T. Bergmark, and K. Siegbahn, *J. Electron Spectrosc. Relat. Phenom.*, **2**, 405 (1974); Y. Baer, G. Busch, and P. Cohn, *Rev. Sci. Instrum.*, **46**, 466 (1975).
(4) M. S. Banna and D. A. Shirley, *J. Elect. Spectrosc. Relat. Phenom.*, **8**, 23 (1976), and references therein.
(5) D. E. Eastman, "Proceedings of the IV International Conference on Vacuum Ultraviolet Radiation Physics", E. Koch, R. Haensel, and C. Kunz, Ed., Pergamon Press, New York, N.Y., 1974.
(6) W. L. Jolly, *Coord. Chem. Rev.*, **13**, 47 (174).
(7) For a discussion of such effects, see L. Ley, R. A. Pollak, F. R. McFeely, S. P. Kowalczyk, and D. A. Shirley, *Phys. Rev. B*, **9**, 600 (1974).
(8) G. M. Bancroft, I. Adams, H. Lampe, and T. K. Sham, *Chem. Phys. Lett.*, **32**, 173 (1975).
(9) G. M. Bancroft, I. Adams, D. K. Creber, D. E. Eastman, and W. Gudat, *Chem. Phys. Lett.*, **38**, 83 (1976).
(10) D. E. Eastman, W. D. Grobman, J. L. Freeouf, and M. Erbudak, *Phys. Rev. B*, **9**, 3473 (1974).
(11) G. M. Bancroft, I. Adams, L. L. Coatsworth, C. D. Bennewitz, J. R. Brown, and W. D. Westwood, *Anal. Chem.*, **47**, 586 (1975).
(12) G. M. Bancroft and T. K. Sham, *Can. J. Chem.*, **52**, 1361 (1974), and references therein.
(13) J. P. Fackler, *Prog. Inorg. Chem.*, **7**, 361 (1966), and references therein.
(14) J. N. R. Ruddick, J. R. Sams, and J. C. Scott, *Inorg. Chem.*, **13**, 1503 (1974), and references therein.
(15) F. A. Cotton and G. Wilkinson, "Advanced Inorganic Chemistry", 2nd ed, Wiley, New York, N.Y., 1966.
(16) R. W. G. Wyckoff, "Crystal Structures", Vol. 1, 2nd ed, Wiley, New York, N.Y., 1963.
(17) J. Berkowitz, *J. Chem. Phys.*, **61**, 407 (1974).
(18) D. J. Kennedy and S. T. Manson, *Phys. Rev. A*, **5**, 227 (1972).
(19) T. E. H. Walker, J. Berkowitz, J. L. Dehmer, and J. T. Waber, *Phys. Rev. Lett.*, **31**, 678 (1973), and references therein.
(20) S. Evans, A. Hammett, A. F. Orchard, and D. R. Lloyd, *Discuss. Faraday Soc.*, **54**, 227 (1972).
(21) W. C. Price, A. W. Potts, and D. G. Streets, "Electron Spectroscopy", D. A. Shirley, Ed., North-Holland Publishing Co., Amsterdam, 1971.
(22) L. Åsbrink, O. Edqvist, E. Lindholm, and L. E. Selin, *Chem. Phys. Lett.*, **5**, 192 (1970).
(23) A. W. Potts, W. C. Price, D. G. Streets, and T. A. Williams, *Discuss. Faraday Soc.*, **54**, 168 (1972), and the following discussion by E. Lindholm (p 200) and W. C. Price (p 205).
(24) U. Gelius, *J. Electron Spectrosc. Relat. Phenom.*, **5**, 1039 (1974).
(25) T. K. Kobayashi and S. Nagakura, *J. Electron Spectros. Relat. Phenom.*, **7**, 187 (1975).
(26) S. Evans, J. C. Green, P. J. Joachim, A. F. Orchard, D. W. Turner, and J. P. Maier, *J. Chem. Soc., Faraday Trans. 2*, 905 (1972).
(27) G. M. Bancroft, K. D. Butler, A. T. Rake, and B. Dale, *J. Chem. Soc., Dalton Trans.*, 2025 (1972).
(28) D. W. Barnum, *J. Inorg. Nucl. Chem.*, **22**, 183 (1961).
(29) G. M. Bancroft, C. Reichert, and J. B. Westmore, *Inorg. Chem.*, **7**, 870 (1968).
(30) S. M. Schildcrout, R. G. Pearson, and F. E. Stafford, *J. Am. Chem. Soc.*, **90**, 4006 (1968).
(31) K. Siegbahn, C. Nordling, G. Johanson, J. Hedman, P. F. Neden, K. Hamrin, U. Gelius, T. Bergmark, L. O. Werme, R. Manne, and Y. Baer, "ESCA Applied to Free Molecules", North-Holland Publishing Co., Amsterdam, 1971.
(32) B. W. Veal, D. J. Lam, W. T. Carnall, and H. R. Hockstra, *Phys. Rev. B*, **12**, 5651 (1975).
(33) F. A. Cotton, "Chemical Applications of Group Theory", 2nd ed, Wiley, New York, N.Y., 1971, p 227.
(34) W. B. Perry and W. L. Jolly, *J. Electron Spectrosc. Relat. Phenom.*, **4**, 219 (1974).
(35) L. E. Cox and D. M. Hercules, *J. Electron Spectrosc. Relat. Phenom.*, **1**, 193 (1973).
(36) E. J. McGuire, Atomic Subshell Photoionization Cross Sections for $2 \leq Z \leq 54$, Sandia Labs Report SC-RR-70-721, Nov. 1970.
(37) G. M. Bancroft, D. E. Eastman, and W. Gudat, *J. Electron Spectrosc., Relat. Phenom.*, in press.
(38) G. K. Wertheim and S. S. Hüfner, *Phys. Rev. Lett.*, **35**, 53 (1975).
(39) S. Doniach and M. Sunjic, *J. Phys. C*, **3**, 285 (1970).
(40) C. J. Ballhausen, "Introduction to Ligand Field Theory", McGraw-Hill, New York, N.Y., 1962.
(41) G. M. Bancroft, I. Adams, T. K. Sham, and H. Lampe, *J. Electron Spectrosc. Relat. Phenom.*, **9**, 191 (1976).
(42) K. Siegbahn, *J. Electron Spectrosc. Relat. Phenom.*, **5**, 3 (1974).
(43) A. Barrie, *Chem. Phys. Lett.*, **19**, 109 (1973).
(44) P. H. Citrin, *Phys. Rev. B*, **8**, 5545 (1973).
(45) S. K. Sen, *Nucl. Instrum. Methods*, **72**, 32 (1969).
(46) R. P. Gupta, B. K. Rao, and S. K. Sen, *Phys. Rev. A*, **3**, 545 (1971).
(47) H. Basch, J. W. Moscowitz, C. Hollister, and D. Hankin, *J. Chem. Phys.*, **55**, 1922 (1971).
(48) (a) F. J. Comes, R. Haensel, U. Neilsen, and W. H. E. Schwartz, *J. Chem. Phys.*, **58**, 516 (1973); (b) G. M. Gancroft, P. A. Malmquist, U. Gelius, and K. Siegbahn, to be published.
(49) B. Bleaney and K. W. H. Stevens, *Rep. Prog. Phys.*, **16**, 108, (1953); M. G. Clark, G. M. Bancroft, and A. J. Stone, *J. Chem. Phys.*, **47**, 4250 (1967).
(50) J. T. Haugen, G. E. Leroi, and T. C. James, *J. Chem. Phys.*, **34**, 1670 (1961).
(51) T. K. Sham and G. M. Bancroft, *Inorg. Chem.*, **14**, 2281 (1975), and references therein.
(52) T. A. Carlson, C. C. Lu, T. C. Tucker, C. W. Neston, and F. B. Malik, Oak Ridge Report ORNL-4614, 1970.
(53) L. Ley, S. P. Kowalczyk, F. R. McFeely, and D. A. Shirley, *Phys. Rev. B*, **10**, 4881 (1974).
(54) G. M. Bancroft, "Mössbauer Spectroscopy: An Introduction for Inorganic Chemists and Geochemists", McGraw-Hill, London, 1973.
(55) G. J. Perlow, "Chemical Application of Mössbauer Spectroscopy", V. I. Goldanskii and R. H. Herber, Ed., Academic Press, New York, N.Y., 1968, p. 377.
(56) R. P. Gupta and S. K. Sen, *Phys. Rev. Lett.*, **28**, 1311 (1972).
(57) R. P. Gupta and S. K. Sen, "Electron Emission Spectroscopy", W. Dekeyser, L. Fiermans, G. Vanderkelen, and J. Vennik, Ed., Reidel, Holland, 1973.
(58) D. A. Shirley, *J. Electron. Spectrosc. Relat. Phenom.*, **5**, 135 (1974).
(59) T. X. Carroll, R. W. Shaw, Jr., T. D. Thomas, C. Kindle, and N. Bartlett, *J.*

Am. Chem. Soc., **96**, 1989 (1974).
(60) U. Gelius, S. Svensson, H. Siegbahn, E. Basilier, Å. Faxlav, and K. Siegbahn, *Chem. Phys. Lett.*, **28**, 1 (1974).
(61) R. C. Poller, "Chemistry of Organotin Compounds", Academic Press, New York, N.Y., 1970.
(62) A. F. Orchard and N. V. Richardson, *J. Electron Spectrosc. Relat. Phenom.*, **6**, 61 (1975).
(63) P. Burroughs, S. Evans, A. Hamnett, A. F. Orchard, and N. V. Richardson, *J. Chem. Soc., Chem. Commun.*, 921 (1974).
(64) P. Citrin, P. Eisenberger, and D. R. Hamann, *Phys. Rev. Lett.*, **33**, 965 (1974).
(65) Y. Baer, P. H. Citrin, and G. K. Wertheim, *Phys. Rev. Lett.*, **37**, 49 (1976).
(66) R. M. Friedman, J. Hudis, and M. L. Perlman, *Phys. Rev. Lett.*, **29**, 692 (1974); R. W. Shaw and T. D. Thomas, *Ibid.*, **29**, 689 (1972).
(67) L. Ley, R. Pollak, S. Kowalczyk, and D. A. Shirley, *Phys. Rev. Lett.*, **41A**, 429 (1972).
(68) G. M. Bancroft, W. Gudat, and D. E. Eastman, in preparation.
(69) R. A. Pollak, S. Kowalczyk, L. Ley, and D. A. Shirley, *Phys. Rev. Lett.*, **29**, 274, (1972).

Aqueous Lanthanide Shift Reagents. 3. Interaction of the Ethylenediaminetetraacetate Chelates with Substituted Ammonium Cations

Gabriel A. Elgavish* and Jacques Reuben

Contribution from the Isotope Department, The Weizmann Institute of Science, Rehovot, Israel. *Received August 26, 1976*

Abstract: The ethylenediaminetetraacetate (EDTA) chelates of the trivalent lanthanides form in aqueous solution ion pairs with organic cations, e.g., substituted ammonium ions, and thereby can act as aqueous shift and relaxation reagents in these systems. By competition, the interaction of inorganic cations with $Ln(EDTA)^-$ can also be studied by ^1H NMR. The pH profiles reveal that at pH values above 8 the hydroxo complex, $Ln(EDTA)(OH)^{2-}$, is formed, which also interacts with cations. The apparent dissociation constant of the $Pr(EDTA)^-$–$(CH_3)_nNH_{4-n}^+$ ion pair decreases with increasing methylation from 0.50 to 0.17 M (at 39 °C) and likewise the intrinsic induced shift decreases from 1.38 to 0.38 ppm. From these results, as well as from the relative broadenings induced by $Gd(EDTA)^-$, it is concluded that in the ion pair one of the methyl groups is closer to the central lanthanide ion than the others. The mean distances between the methyl protons and the gadolinium were calculated from the intrinsic line widths. The values obtained for acetate, methylammonium, and tetramethylammonium are 5.3, 7.7, and 10.3 Å, respectively. The interaction with $Yb(EDTA)^-$ is very weak. This is in agreement with a previously suggested model for the structure of $Ln(EDTA)^-$ chelates in solution, which assumes that the lighter lanthanides are pentachelated and have a free acetate arm capable of interacting with cations. On the other hand, the heavier lanthanides are hexachelated and lack such an ability.

The suitability of the ethylenediaminetetraacetate (EDTA) chelates of the trivalent lanthanides as aqueous shift and relaxation reagents for carboxylate and chelating phenolate substrates has recently been established.[1,2] It might be intuitively anticipated that the $Ln(EDTA)^-$ chelates, by virtue of their negative charge, would interact with cations in solution. Indications for such interactions have been obtained from the effects of LiCl concentration upon the observed shifts in the acetate–$Ln(EDTA)^-$ systems.[1] Presented in this article are the results of our studies on the interaction of substituted ammonium cations with $Pr(EDTA)^-$, which is a shift reagent, and with $Gd(EDTA)^-$, which is a relaxation reagent. Some experiments with the weakly interacting $Yb(EDTA)^-$ were also carried out. Details of the pH dependence of the induced shifts and line broadening, of the chemical equilibria, and of the structure of the complexes were elucidated. Additional evidence was obtained supporting our ideas[1] regarding the nature of the structural change of the EDTA chelates along the lanthanide series.

Experimental Section

Solutions of the $Ln(EDTA)^-$ chelates were prepared and analyzed as previously described.[1] Analytical grade substituted ammonium chlorides of the free amines were used. The latter were employed in the study of the pH dependence. The highest pH investigated was attained by the addition of LiOD and the solution was then titrated with DCl. Reported pH values are meter readings corrected for deuterium isotope effects.

Proton NMR spectra were recorded on a Varian T-60 spectrometer operating at the ambient probe temperature of 39 ± 1 °C. A small amount of *tert*-butyl alcohol, ca. 0.1% v/v, served as an internal standard.

Results

The effect of $Pr(EDTA)^-$ on the proton spectrum of the pyridinium cation is depicted in Figure 1. In contrast with the line overlap in the spectrum of pyridinium, the paramagnetic perturbation results in distinct and readily assignable multiplets. In particular H_2 is shifted downfield by 0.3 ppm from its diamagnetic position.

Depending upon the relative concentrations of hydrogen or hydroxyl ions, either protonation[3] or formation of hydroxo complexes[1] of the $Ln(EDTA)^-$ chelates may occur. In addition, the ammonium cations, except for tetramethylammonium (TMA), undergo deprotonation at high pH. It is therefore imperative to investigate the pH profile of the induced shifts and line broadenings in this system. The pH profiles of the downfield shifts induced by $Pr(EDTA)^-$ in the proton resonances of methylammonium (MA) and TMA are shown in Figure 2. Also shown are the shifts in the absence of shift reagent. The shifts of MA are referred to the diamagnetic deprotonated base and those of TMA to its diamagnetic position. The induced shift for MA approaches zero at high pH indicating that methylamine interacts neither with $Pr(EDTA)^-$ nor with its hydroxo complex. On the other hand, for TMA a sign reversal of the induced shift is observed above pH 11. This indicates, as might be intuitively anticipated, that TMA interacts with $Pr(EDTA)(OH)^{2-}$. Referring to the dipolar shift relation

$$\delta_M = C(3\cos^2\theta - 1)/r^3 \quad (1)$$